

PARAMETERS OF A LARGE BUBBLE CHAMBER

R. Kraemer
Carnegie-Mellon University

and

M. Derrick
Argonne National Laboratory

January 6, 1969

The FAKE-GRIND programs now operate as a useful package for simulating and fitting events in the 12-ft and the 25-ft chambers. By considering momentum and angle errors,¹ it is shown that the optimum length of a track such that the angle error is a minimum, with equal contributions from the scattering and measuring errors, is 4 to 6 meters for the momentum range 30 to 100 GeV/c, for realistic setting errors of 250 and 500 μ for the 12-ft and the 25-ft chambers. Plots indicating the different contributions to $\Delta p/p$, the variation with $(\Delta p/p)_{\text{total}}$ and $(\Delta\theta)$ with p for the ANL 30-in., BNL 80-in., and the 12-ft and 25-ft chambers are presented. For example, for $\Delta p < 100$ MeV/c the 25-ft chamber can go up to 55 GeV/c, the 12-ft up to 35 GeV/c (both with a 40-kG field). However for the multiplicities expected at high energy only a small fraction of secondaries will not interact, and the actual momentum resolution will be considerably increased. Errors in the effective mass of two particles are shown to be comparable to

those presently obtainable, over a fairly wide range. (Most of this work has been previously discussed by Fisher.¹⁾)

Scaling of Momentum and Angle Errors

A twofold attack was used to study this problem. First, we decided to make the Monte Carlo program "FAKE" and the kinematics program "GRIND" work as a complete package. Progress was such that the system is now a useful tool. Second, hand calculations based on standard error parameters were made to provide orientation and to determine such quantities as optimum path length and optimum magnetic field. We were also able to draw some conclusions on the basis of these calculations.

FAKE-GRIND

The system now produces useful output. Both the 12-ft and the 25-ft chambers are simulated and events of most types may be generated by FAKE and run through GRIND.

As a program for the future we plan an extensive study of neutrino-induced reactions and strong interactions involving resonance production. A crucial question is whether any conclusive strong-interaction physics can be done in the 25-ft chamber. Another pressing question has to do with high-energy neutrino physics. For "elastic" events we want to know how often we will also get a fit to a missing π^0 . Since the neutrino momentum is not known it is clear that a single

forward-going neutral pion will be difficult to exclude. We will also examine N* production to see how often and under what kinematic conditions N* production is faked by an "elastic" event. All of these questions relate to the problem of detection of neutral particles in high-energy interactions.

Simple Hand Calculations

Formulas for momentum and angle errors have been given by Fisher.¹

They are

$$\left(\frac{\Delta p}{p} \right)^2 = \frac{0.133\alpha}{H^2 l} + \frac{1.44 \cdot 10^{-4} p^2 e^2}{H^2 l^5}, \quad (1)$$

$$(\Delta \sigma)^2 = \frac{2 \cdot 10^{-3} \alpha l}{p^2} + \frac{3.8 \cdot 10^{-6} e^2}{l^3} \quad (2)$$

$$\text{where } \alpha = \ln 4.8p + \ln 145 p/H. \quad (3)$$

Now, α is a slowly varying function of p which we take equal to 20.

Tracks are assumed to be flat (dip angle = 0°) and units are

H (kG),

p (MeV/c),

e (microns in space),

l (cm), and

θ (radians).

As can be seen from (2), there is an optimum length condition for angles

such that for a fixed-setting error, ϵ , and fixed momentum, scattering dominates for $L > L_{\text{opt}}$ and measuring dominates for $L < L_{\text{opt}}$. The optimum length is given by:

$$\ell_0 = 0.1 (p\epsilon)^{\frac{1}{2}}. \quad (4)$$

For this track length the angle errors are a minimum. In Fig. 1, we plot optimum length vs momentum with ϵ as a parameter. On the same plot, we show length vs momentum for the condition $(\Delta p/p)_{\text{coulomb}} = (\Delta p/p)_{\text{measurement}}$. This gives $\ell_1 = 0.085 (p\epsilon)^{\frac{1}{2}}$. It is clear that for the optimum angle measurement condition, momentum measurements are coulomb scattering limited. In that case, Eq. (1) says it is more efficient to increase the magnetic field rather than the track length.

The lengths shown in Fig. 1 are of the order of a few meters for momenta in the range 30 GeV/c to 100 GeV/c and setting errors between 100μ and 500μ which is appropriate to the size of the chambers being discussed. As an appendix to this report we include an Argonne note² about the expected reconstruction accuracy in the 12-ft chamber. Probably 250μ is a number that can be achieved with some work. Thermal turbulence in the chamber dominates this error. For the same heat flux the 25-ft chamber will be about 3 times worse because of the extra depth of the chamber. Then 500μ is an optimistic value of ϵ for the 25 ft.

Figure 2 shows the contribution to $\Delta p/p$ from measuring error for $H = 20$ kG and $\epsilon = 250\mu$ as a function of track length for different momenta. The curves are the same for $H = 40$ kG and $\epsilon = 500\mu$ which are more appropriate to the 25-ft chamber.

Figure 3 shows the contribution to $(\Delta p/p)$ from multiple scattering.

The circled points in Figs. 2 and 3 illustrate that for 50 GeV/c the momentum errors are matched at 4.3 m (with $\epsilon/H = 10$). Simultaneously, the angle errors are approximately matched.

Next, in Fig. 4 we show $(\Delta p/p)_{\text{total}}$ vs momentum for the ANL 30-in., BNL 80-in., 12-ft and 25-ft chambers. Optimum lengths and realistic setting errors have been chosen. At low momentum, scattering dominates while at high momentum the measurement error takes over and increases as p . Also plotted are lines of constant Δp of 25, 50, 100, and 200 MeV/c.

From experience with present-day chambers, we know that good discrimination for 4c events is possible in the ANL 30-in. chambers between 5 GeV/c and 7 GeV/c and in the BNL 80-in. up to 15 GeV/c. The 100 MeV/c-200 MeV/c lines then indicate the upper momenta for similar precision in the new chambers. We see that for the 25-ft chamber the region of 30-90 GeV/c is contained within $\Delta p = 50$ -200 MeV/c. In the same region, the measuring and scattering errors are roughly equal. If one wanted to hold $\Delta p < 100$ MeV/c, one can see that the 25-ft chamber would do this for up to 55 GeV/c tracks whereas

the 12-ft chamber with 20 kG would cut out at 20 GeV/c momentum.

If the 12-ft chamber were equipped with a 40 kG magnet (a possibility that is very much in the range of present technology), then the upper limit for $\Delta p = 100 \text{ MeV/c}$ goes from 20 GeV/c to 35 GeV/c, a very significant improvement. The track lengths chosen for these calculations are given in Fig. 4 and are reasonable considering one needs a fiducial volume in the chamber. Secondary-particle interactions will reduce these lengths as discussed in the next section.

Figure 5 is a slightly different version of Fig. 4. Here we display $(\Delta p/p)$ vs momentum and show the variation of $(\Delta p/p)$ as the setting error changes and the field and length are held constant.

Figure 6 shows $\Delta\theta$ vs momentum where applicable. Here we have chosen optimum lengths and realistic setting errors. The angle errors fall to $\sim 0.1 \text{ mrad}$ s, approximately following a fixed Δp_{\perp} line. To realize this accuracy, it will be necessary to keep the setting error precision independent of the position in the chamber, i. e., two points several meters apart will need to be known relative to each other to an accuracy of a few hundred microns.

Particle Multiplicity

At high incoming momenta, high multiplicity is expected. For

example, in p-p collisions, Hagedorn and Ranft³ predict at 300 GeV/c a multiplicity of 6 charged particles, and cosmic-ray data lie between 8 and 10. The predicted multiplicity at 30 GeV/c is about 5 particles and compares very favorably with experiment. So we can make a very good guess as to multiplicities at 100-200 GeV/c. We have calculated, in the same manner as Fisher,¹ the following tables:

Table I. Fraction of Events In Which All Tracks Survive Length L, Without Interacting for an Interaction Cross Section Of 25 mb ($\lambda = 1100$ cms). All Tracks Are Assumed To Have the Same Length.

L (cm) \ Charged Multiplicity	2	4	6	8
100	0.82	0.67	0.55	0.45
200	0.69	0.48	0.33	0.23
400	0.49	0.24	0.12	0.06
600	0.34	0.12	0.04	0.01

Table II. Same as Table I but with $\lambda = 550$ cm ($\sigma = 50$ mb) Appropriate to a Deuterium Filling of the Chamber.

L (cm) \ Charged Multiplicity	2	4	6	8
100	0.70	0.49	0.34	0.25
200	0.49	0.25	0.12	0.06
400	0.25	0.06	0.015	0.004
600	0.12	0.01	10^{-3}	10^{-4}

Table III. Fraction of Events In Which One Track Interacts In Length L, and All Others Survive. All Tracks Are Taken To Be Identical and $\lambda = 550$ cm.

L(cm)	Multiplicity			
	2	4	6	8
100	0.28	0.38	0.27	0.37
200	0.42	0.41	0.31	0.19
400	0.50	0.24	0.09	0.03
600	0.45	0.11	0.02	0.003

Now we have a real dilemma. First, we advertise that we need 4-6 meters of path length to do 4c physics at 60 GeV to 90 GeV and then discover that for the multiplicities expected only a small fraction of the events will have no interacting secondaries.

As a simple example, we take 100 GeV/c incident and 4 outgoing particles ($\lambda = 1110$ cm). Now at 2 meters, 50% of events will suffer no secondary interactions. However, $\Delta p/p$ for a 25 GeV/c track having $L = 200$ cm in the 25-ft chamber with 40 kG is about 6×10^{-3} or $\Delta p = 150$ MeV/c. At 50 GeV/c the Δp is about 500 MeV/c. So, unless one is willing to throw away a large sample of events, the 25-ft chamber ends up looking like a much smaller chamber from the point of view of momentum resolution. The secondary vertices will

not often be 4-constraint and so not of much use with regard to kinematic fitting, although in some cases they will give important qualitative information. For example, if the secondary interaction gives a V^0 , the track giving that interaction is more likely to be a K meson than a π meson.

Effective Mass Resolution

At high momentum, we can write for the effective mass of two outgoing particles (M_1 and M_2)

$$\frac{\Delta M}{M} = \frac{Q^2}{M^2} \left\{ \frac{1}{2} \left(\frac{\Delta p}{p} \right)^2 + \left(\frac{\Delta \sigma}{\sigma} \right)^2 \right\}^{\frac{1}{2}},$$

where $Q^2 = M^2 - M_1^2 - M_2^2 = p^2 \theta^2$. We have chosen the symmetric case $p_1 = p_2 = p$. θ is the opening angle. Making use of the relation $L_{\text{opt}} = 0.1 (p\epsilon)^{\frac{1}{2}}$ we find

$$\left(\frac{\Delta \sigma}{\sigma} \right)^2 = \frac{8 \times 10^{-3}}{Q^2} (p\epsilon)^{\frac{1}{2}}$$

$$\left(\frac{\Delta p}{p} \right)^2 = \frac{41}{H^2 (p\epsilon)^{\frac{1}{2}}}.$$

We now ask an interesting question. How big should the magnetic field be in order to have equal contribution to the error on effective mass from the momentum errors and the angle errors?

Putting

$$\left(\frac{\Delta\sigma}{\sigma}\right)^2 = \frac{1}{2} \left(\frac{\Delta p}{p}\right)^2,$$

we find the simple relation

$$p = \frac{2.6 \times 10^3 Q^2}{\epsilon H^2},$$

where the units are p (MeV/c), ϵ (μ in space), H (kG), and Q (MeV).

Thus, for fixed ϵ and Q we are able to find the optimum magnetic field for matching angle and momentum errors as a function of outgoing-particle momentum. We display this information in Figure 7.

One can see that for a chamber field of 40 kG and ϵ of 500 μ , a $Q = 3$ GeV resonance will have matched errors at momenta of about 35-40 GeV/c. Also shown are curves for $Q = 10$ GeV and 15 GeV which are appropriate to elastic scattering at about 50 GeV/c and 125 GeV/c. These give lab momenta of $50/2 = 25$ GeV/c or $125/2 = 62$ GeV/c and so would require magnetic fields over 100 kG to match the errors. For 40 kG the momentum error still dominates the situation. Figure 8 shows the contribution to $(\Delta M/M)^2$ from angle and momentum errors as a function of momentum. Again, recall that Figs. 7 and 8 make use of the optimum length condition.

As an example of magnitudes involved, we calculate ΔM for $K^0 \rightarrow 2\pi$ decay at 100 GeV/c. We assume optimum length, $H = 40$ kG, and $\epsilon = 500\mu$. The equal momentum configuration has $p = 50$ GeV/c

and $\theta = 0.5^\circ$.

$$\Delta M = \frac{p^2 \sigma^2}{M} \left\{ \frac{1}{2} \left(\frac{41}{M^2 (p\epsilon)^{\frac{1}{2}}} \right) + \left(\frac{8 \times 10^{-3} (p\epsilon)^{\frac{1}{2}}}{p^2 \sigma^2} \right) \right\}^{\frac{1}{2}},$$

where $(p\epsilon)^{\frac{1}{2}} = 5 \times 10^3$ and $p^2 \sigma^2 = 2 \times 10^5$.

Then, $\Delta M \sim 6$ MeV which is very reasonable and in fact comparable to the values obtained at present energies. Recall that $L_{\text{opt}} = 0.1 (p\epsilon)^{\frac{1}{2}} = 500$ cm for the above case. So we are asking that each track have a length of 5 meters. For track length of 2 meters we get $\Delta M = 25$ MeV. In Fig. 9 we show ΔM vs H for p-p scattering at 100 GeV/c. Again we choose the symmetric configuration and we show curves for $\epsilon = 500\mu$, length = 5 m and $\epsilon = 100\mu$, length = 2.3 m. These curves are rather similar indicating that a smaller high precision chamber is quite good. Note that ΔM becomes very large for the case of $\epsilon = 500\mu$ and length = 2 meters.

Argonne National Laboratory
Argonne, Illinois 60439

LIMITS OF RACK LOCATION DETERMINATION IN THE 12-FT HBC

L. R. Turner

July 7, 1967

ANL-BBC-110

I. Results

This note considers the several effects in the 12-ft chamber which will limit the relocation of tracks in the chamber. Table I shows the sources of uncertainty, the expected precision in relocation, and the assumptions under which it is calculated. Figure 1 shows the total deviation compounded with measuring error.

Table I
Limits on Bubble Relocation

Source	Assumptions	Deviation (microns)
Turbulence		
optical	200 cm distance, 10^{-3} Watt/cm ² heat flux	100 to 380
random velocity	2 msec flash delay	160
motion during flash	30 msec period, 2 msec flash delay, 0.2 msec flash duration	170
Temperature Gradient	$\Delta T = 2$ millidegree	7
Pressure Gradient	$\Delta p = 3.3$ psi	44
Fisheye Windows		
misalignment	100 μ misalignment	100
refractive index	$\Delta T = 4^\circ/\text{cm}$; $dn/dT = 5 \times 10^{-6} \text{ deg}^{-1}$	74
change of shape	$\alpha = 1.6 \times 10^{-6} \text{ deg}^{-1}$	4
Vibration	200 μ sec flash duration	16
Film Distortion	1 μ on film	60
Film Flatness	flat to within 20 μ	40
Total Deviation	added in quadrature	300 to 470

II. Turbulence

A. Optical Effects

As discussed in ANL-BBC-22, thermal turbulence in the chamber will produce random temperature fluctuations in the chamber with resulting fluctuations in refractive index. The expected deviation of a bubble relocation is:

$$\delta = d^{3/2} (3\lambda)^{-1/2} \theta_{rms} \quad (1)$$

where d is the distance from the bubble to the window (taken to be 200 cm),

λ is the scale of the turbulence

θ_{rms} is the rms angle of scattering by a fluctuation.

$$\theta_{rms} = 2(n-1) [-\ln(n-1) - 0.807]^{1/2} \quad (2)$$

where n is the ratio of the refractive index in the fluctuation to the average refractive index.

$$\text{We take } n - 1 = \frac{dn}{dT} T_{rms} \quad (3)$$

with $dn/dT = 2.0 \times 10^{-3} \text{ deg}^{-1}$, and T_{rms} the rms variation in temperature.

The rms temperature fluctuation can be predicted on the basis of a Rutherford Laboratory report by D. B. Thomas (AP/DS/HFC/5), in which he summarizes and applies earlier experimental and theoretical results. From the experimental results of Thomas and Townsend, we find

$$T_{rms} = 0.1 T \theta_o \quad (4)$$

$$\lambda = 10 \pi Z_o \quad (5)$$

where T is the absolute temperature

Z_o is a characteristic length

θ_o is a characteristic nondimensional temperature.

For a heat input of $10^{-3} \text{ watt/cm}^2$ (100 watt total heat into fiducial volume), we obtain

$$\theta_o = 0.78 \times 10^{-4}$$

$$Z_o = 1.5 \times 10^{-2} \text{ cm}$$

$$\lambda = 0.49 \text{ cm}$$

$$T_{\text{rms}} = 1.14 \times 10^{-3} \text{ deg}$$

$$n - 1 = 2.3 \times 10^{-6}$$

and finally

$$\delta = 380 \mu. \quad (6)$$

However, Thomas suggests that the experimental results can be extrapolated by a power of distance from $100 Z_0$ ($= 1.5 \text{ cm}$) to the center of the chamber (100 cm). Such an extrapolation yields $\delta = 40 \mu$.

Pictures taken through 60-cm of hydrogen with the 2-ft model chamber show less than 30μ of deviation. Scaling to 200 cm by Eq. (1) yields a deviation of less than 180μ . Thus, 100μ to 380μ might be taken as a range of the deviation. Finally, the deviation δ is proportional to the seven-eighths power of the heat flux.

B. Velocity Effects

Experimental and theoretical results by Malkus, quoted by Thomas, predict that the chamber hydrogen will have random velocities of 8 cm/sec . A flash delay of 2 msec will produce a displacement of 160μ . Malkus' observations suggest that most of this displacement may be associated with large scale motions.

C. Non-Random Velocity Effects

For a one percent expansion with a period of 30 msec, the hydrogen near the bottom of the chamber will have a velocity of recompression $v = 7.21 \sin(206 t) \text{ ft/sec}$. After a flash delay of 2 msec, the velocity will be 2.88 ft/sec . At this velocity, the bubble will move 170μ during a $200 \mu \text{ sec}$ flash duration. In addition the hydrogen will have moved 870μ during the 2 msec, but this motion will not affect the reconstruction of tracks.

III. Temperature and Pressure Gradients Across Chamber

For heat convection across the chamber, the temperature gradient is almost entirely in the boundary layer; the gradient across the bulk of the hydrogen is expected to be a few millidegrees. Using the method of Fetkovich (see BBC-11) we obtain $\delta = 7 \mu$.

The same method can be used to find the deviation due to the 3.3 psi pressure difference across the chamber at maximum expansion. At 45° from the vertical, $\Delta\theta = \Delta n/n = 0.097 \Delta\rho/\rho = 0.097 \Delta p/B = 44 \times 10^{-6}$. At a distance of 200 cm, this will produce a deviation of

$$\delta = \Delta\theta d/2 = 44 \mu .$$

Since the pressure varies smoothly along the chamber, the net effect of this deviation will be negligible.

IV. Fisheye Windows

A. Alignment

As shown in BBC-78, Fig. 2, after uniform displacement and magnification are subtracted the distortion introduced by a misalignment of a fish-eye window is about equal to the misalignment. Thus, a misalignment of 100μ (which is realizable) will produce a distortion of about 100μ . This distortion (like those discussed below) is smoothly varying: Thus much of it may be corrected for in reconstruction if needed.

B. Refractive Index Variation with Temperature

The "room temperature" fisheye and the intermediate fisheye will have temperature gradients of up to 4 deg/cm and more. The refractive index variation is expected to be about $dn/dT = 5 \times 10^{-6} \text{ deg}^{-1}$.

A 2-cm thick window will deflect a light ray by

$$\theta = \frac{1}{n} \frac{dn}{dT} \frac{dT}{dX} L = 27 \mu \text{ radian.}$$

In hydrogen, ($n = 1.1$) the deviation will be 37μ radians, producing a deviation 200-cm away of 74μ .

C. Thermal Stresses in the Fisheye

The temperature differences in the fisheyes will cause them to distort from their spherical shape. The combined effect of thermal and elastic stresses is under study; however, an estimate for the effect of the change in shape can be obtained by assuming each conical element of the fisheye to expand freely. A ray traced through such a window (with $\Delta T = 4 \text{ deg/cm}$, $\alpha = 1.6 \times 10^{-6} \text{ deg}^{-1}$) experiences a displacement after 200 cm of 4μ .

V. Other Effects

A. Vibration

In the M. W. Kellogg report on chamber stresses, a pressure of 165 psi produced at the window location a displacement of 0.016 in. and rotation of 0.05° . With the planned expansion stroke and period, this would predict a blur of $3\ \mu$ due to displacement and $13\ \mu$ due to rotation during the flash duration of $200\ \mu$ sec.

B. Instability of Film

As discussed in BBC-63, distortion on film is expected to be about $1\ \mu$, corresponding to about $60\ \mu$ in space.

C. Non-Flatness of Film

The lens is to be telecentric to within 2° over most of the field. A film non-flatness of $20\ \mu$ would result in $0.7\ \mu$ distortion on the film; $40\ \mu$ in space.

LRT:met

Attachments: Figure 1

Distribution: Standard ANL-BBC Memo List

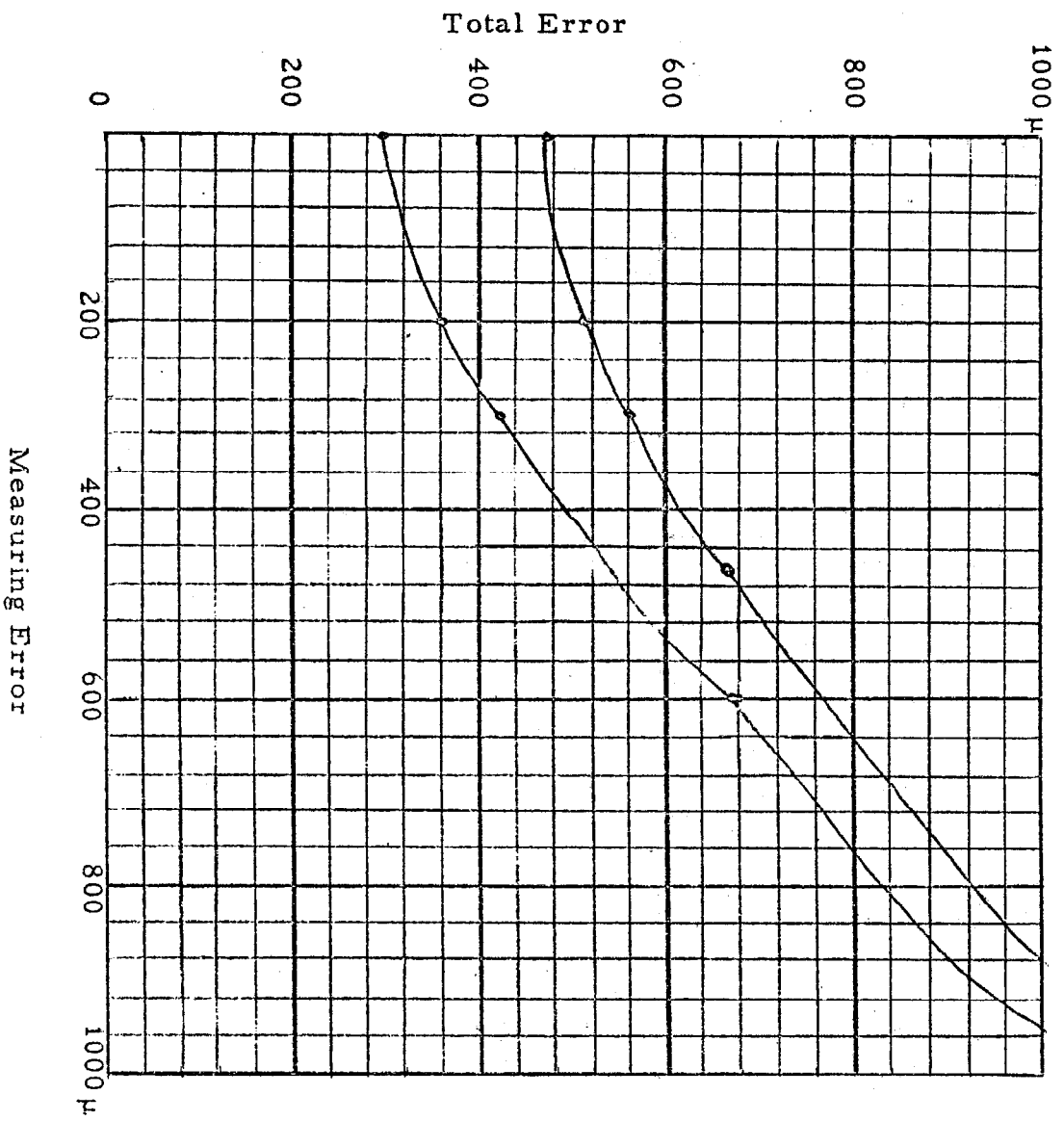


Fig. 1 Total Error vs Measuring Error for Two Estimates of Non-Measuring Error

REFERENCES

- ¹C. M. Fisher, Optimization of Bubble-Chamber Design Parameters, Proc. International Colloquium on Bubble Chambers, CERN, 67-26, 1967, p. 25.
- ²L. R. Turner, Limits of Track Location Determination in the 12-ft HBC, ANL-BBC-110, unpublished (included as an appendix to this report).
- ³R. Hagedorn and J. Ranft, Utilization Studies for a 300-GeV Proton Synchrotron, CERN/ECFA 67/16, Vol. I, 1967, p. 69.

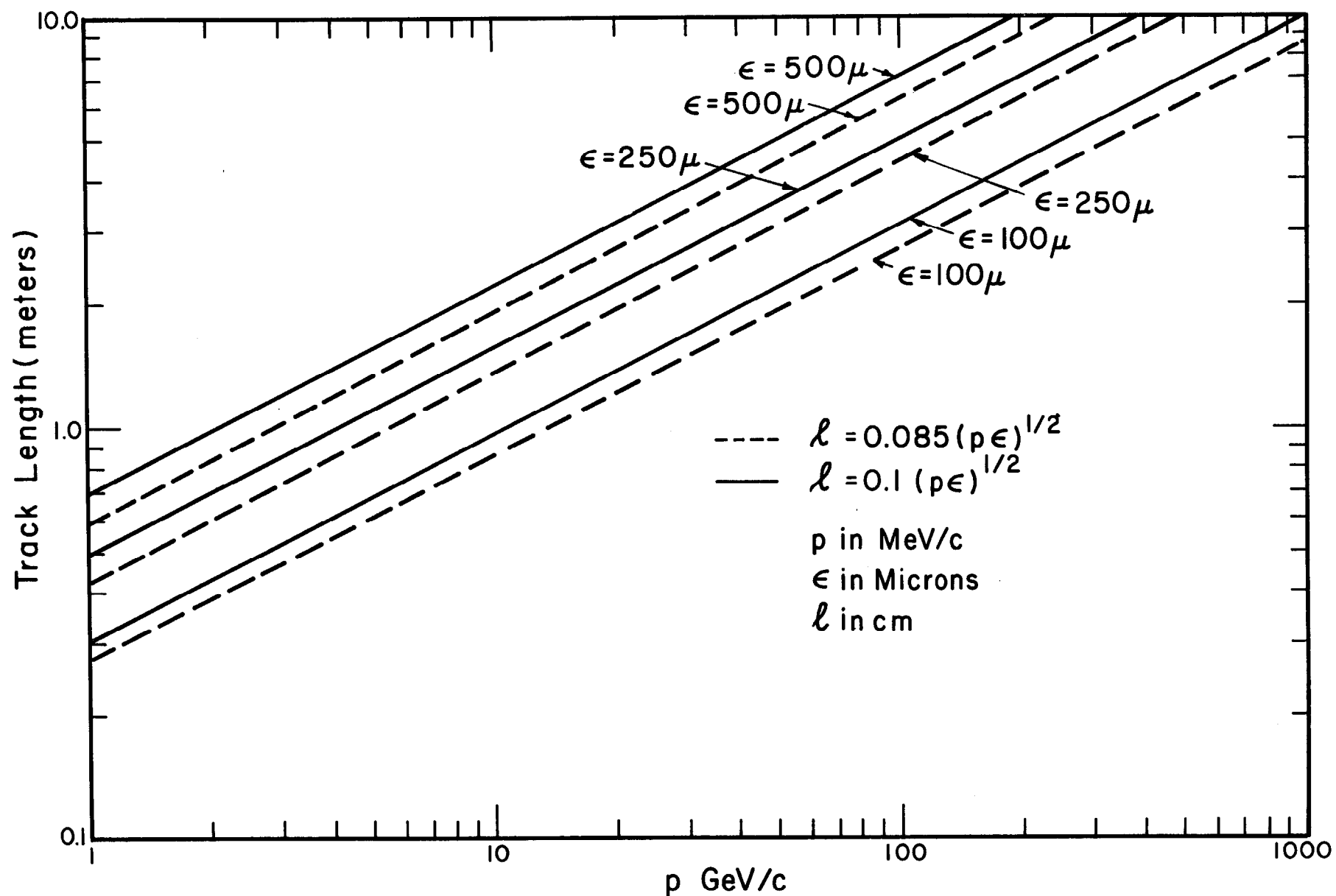


Fig. 1. Optimum track length for angle measurements, assuming measuring and multiple scattering contributions to $\Delta p/p$ equal.

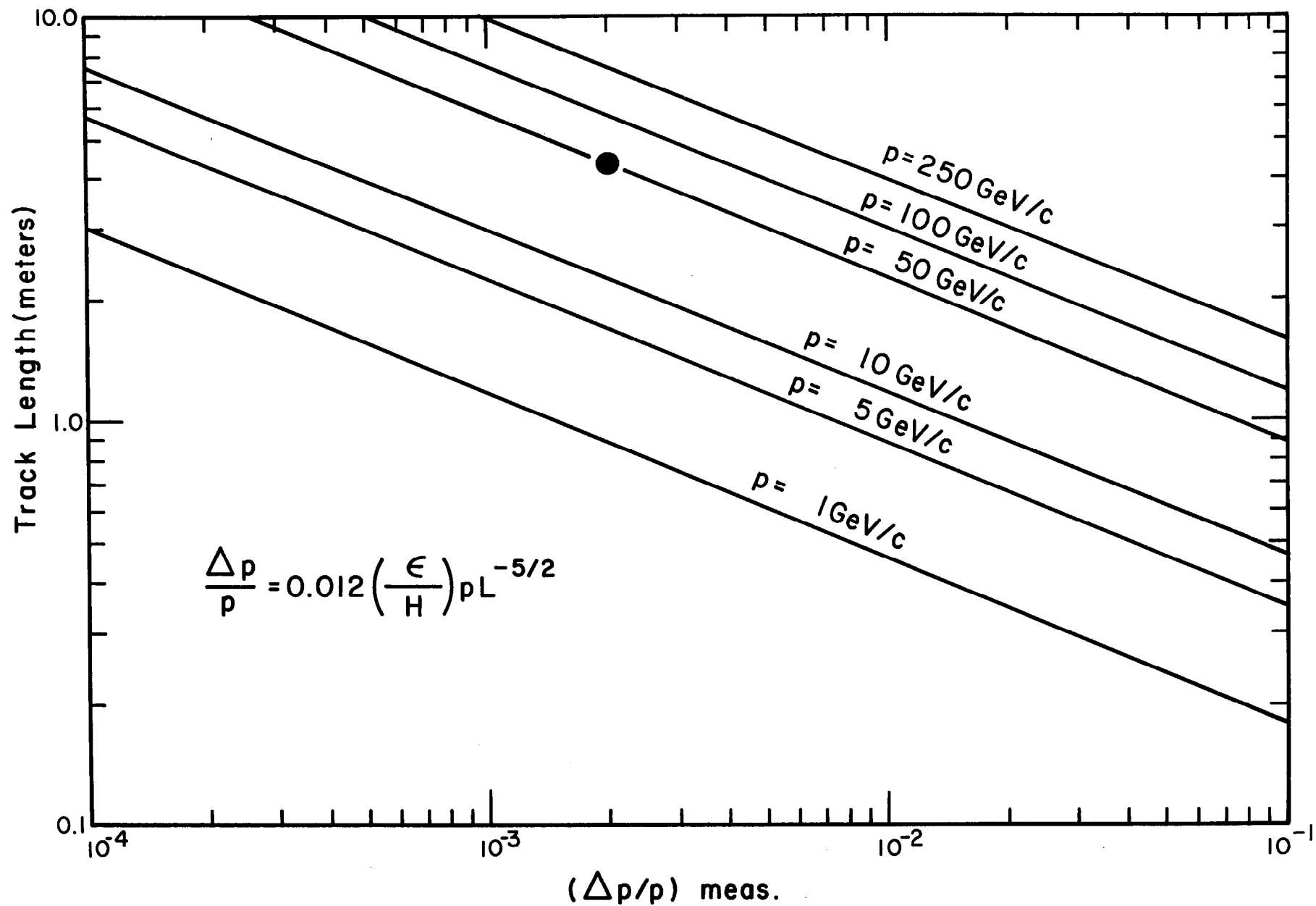


Fig. 2. Contribution to $\Delta p/p$ from measuring error as a function of track length, for

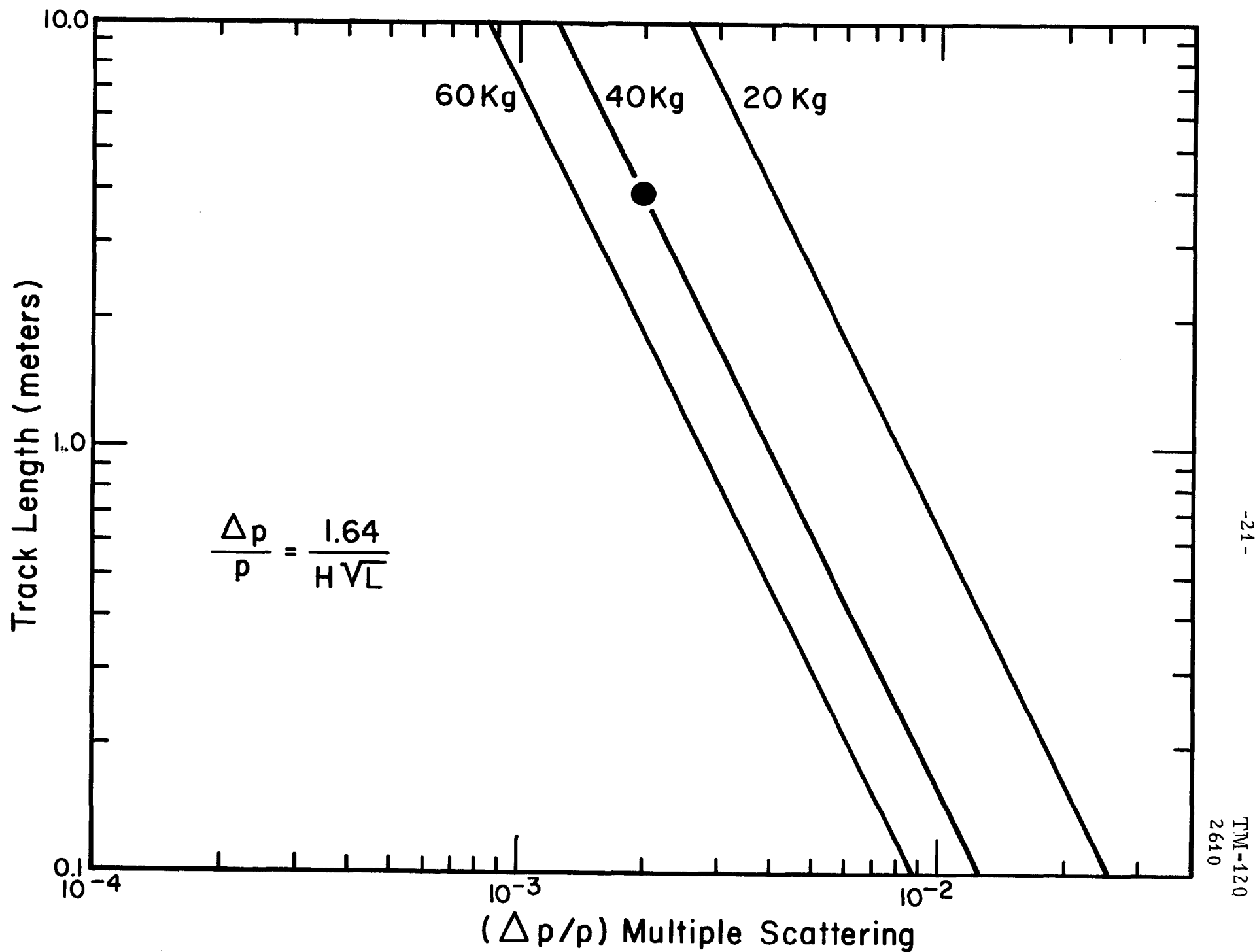


Fig. 3. Contribution to $\Delta p/p$ from multiple scattering, as a function of

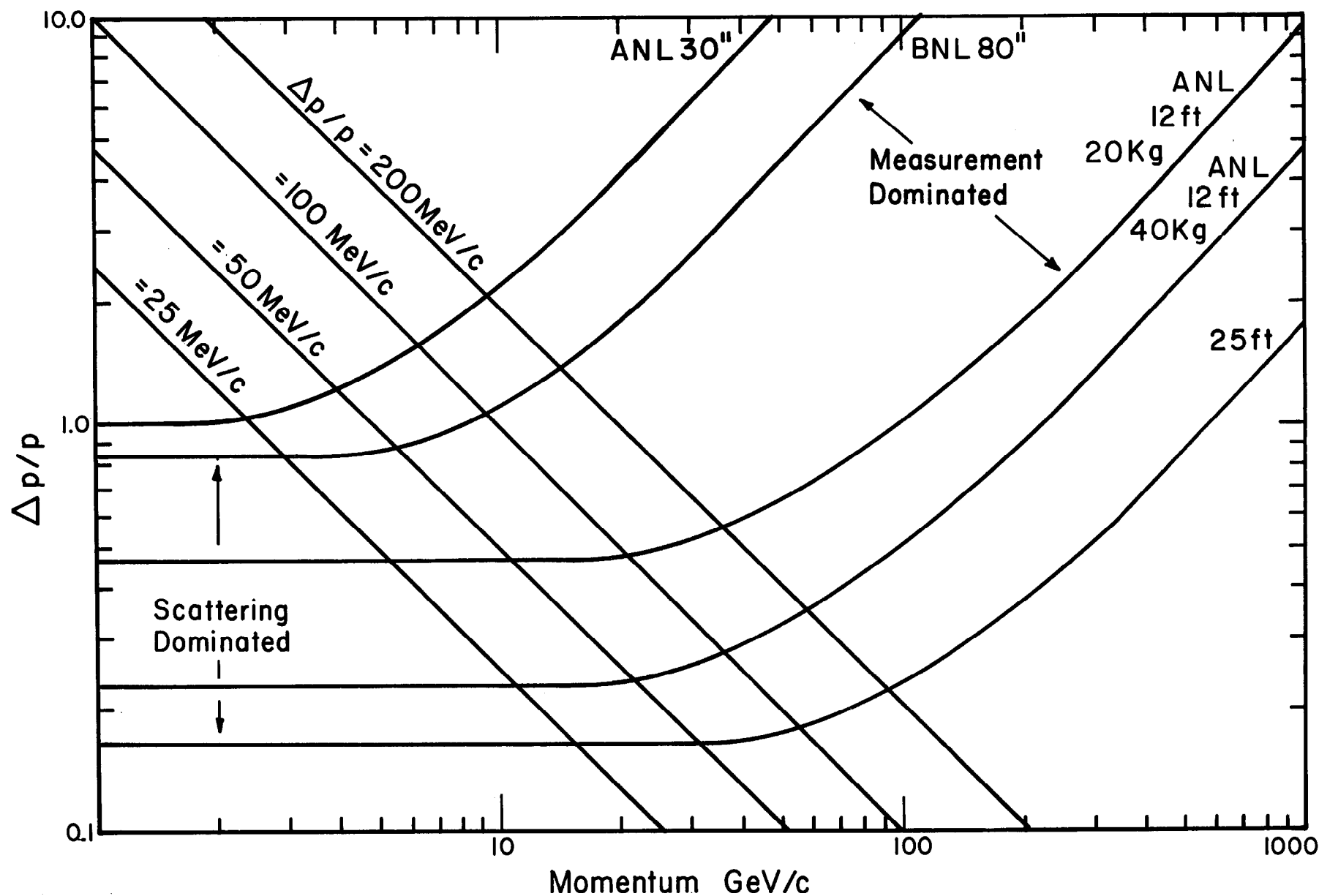


Fig. 4. Total momentum error $\Delta p/p$, for four different bubble chambers. The parameters assumed are: ANL 30", 50-cm track, 100- μ setting error, 32-kgauss field; BNL 80", 100-cm track, 150- μ setting error, 20-kgauss field; ANL 12-ft, 300-cm track, 250- μ setting error, 20- or 40-kgauss field; and BNL 25-ft, 600-cm track, 500- μ setting error, and 40-kgauss field.

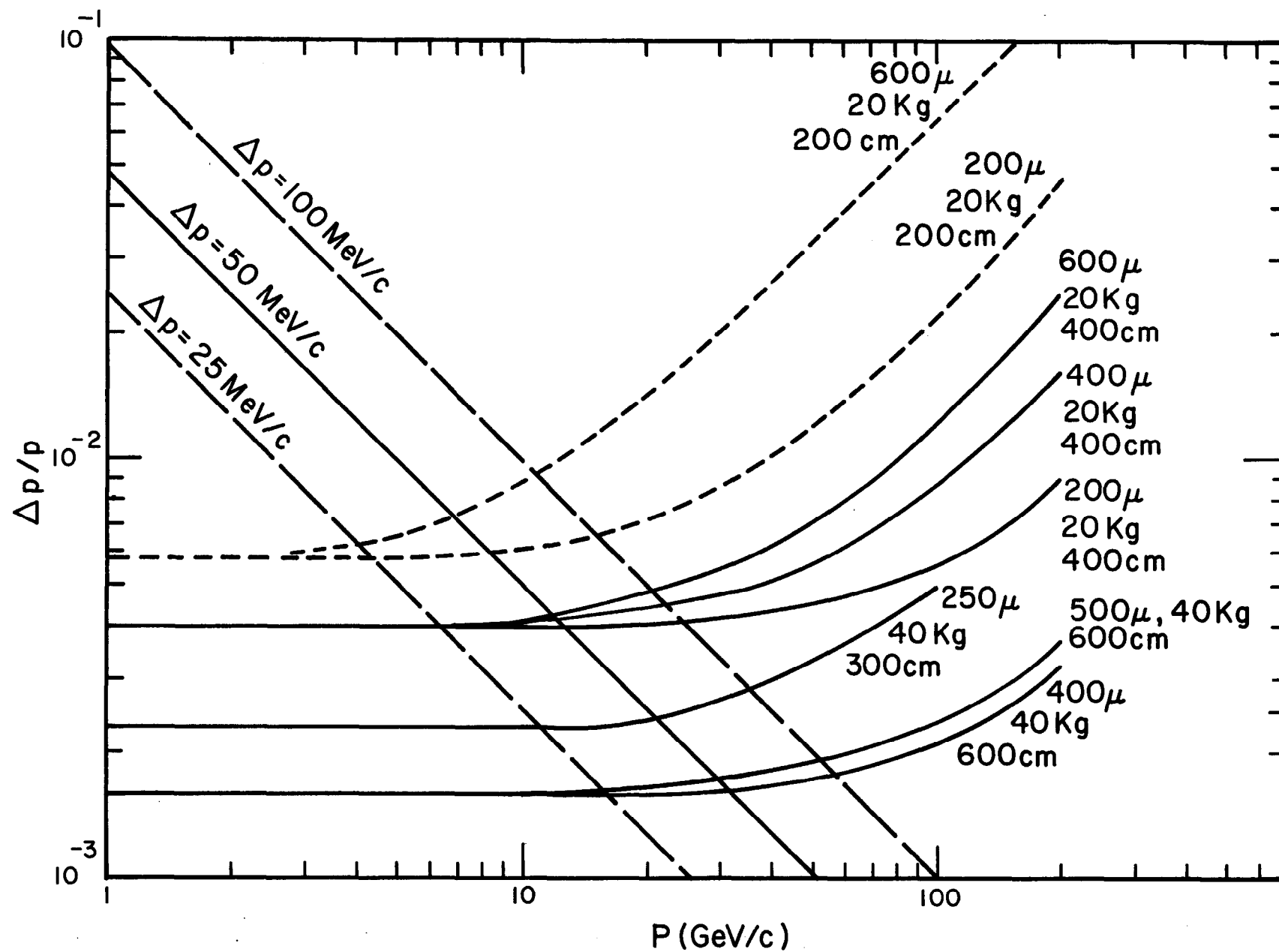


Fig. 5. Effect of varying the setting error on the total momentum error, for the same four bubble chambers

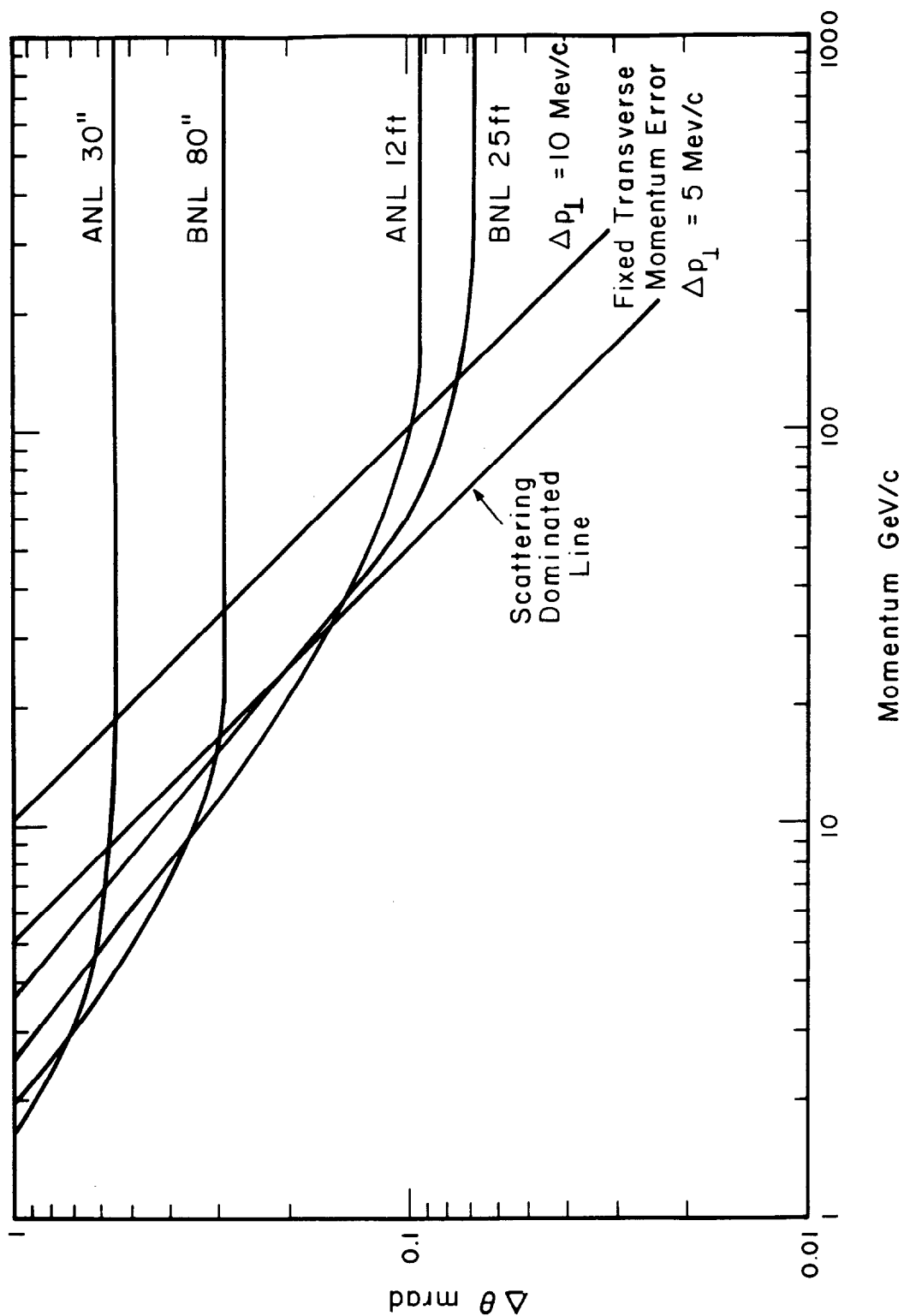


Fig. 6. Angular error vs momentum. Setting errors as in Fig. 4; track lengths 50, 100 cm for ANL 30", BNL 80" chambers, and 300, 600 cm for 12-ft (except optimum lengths when applicable).

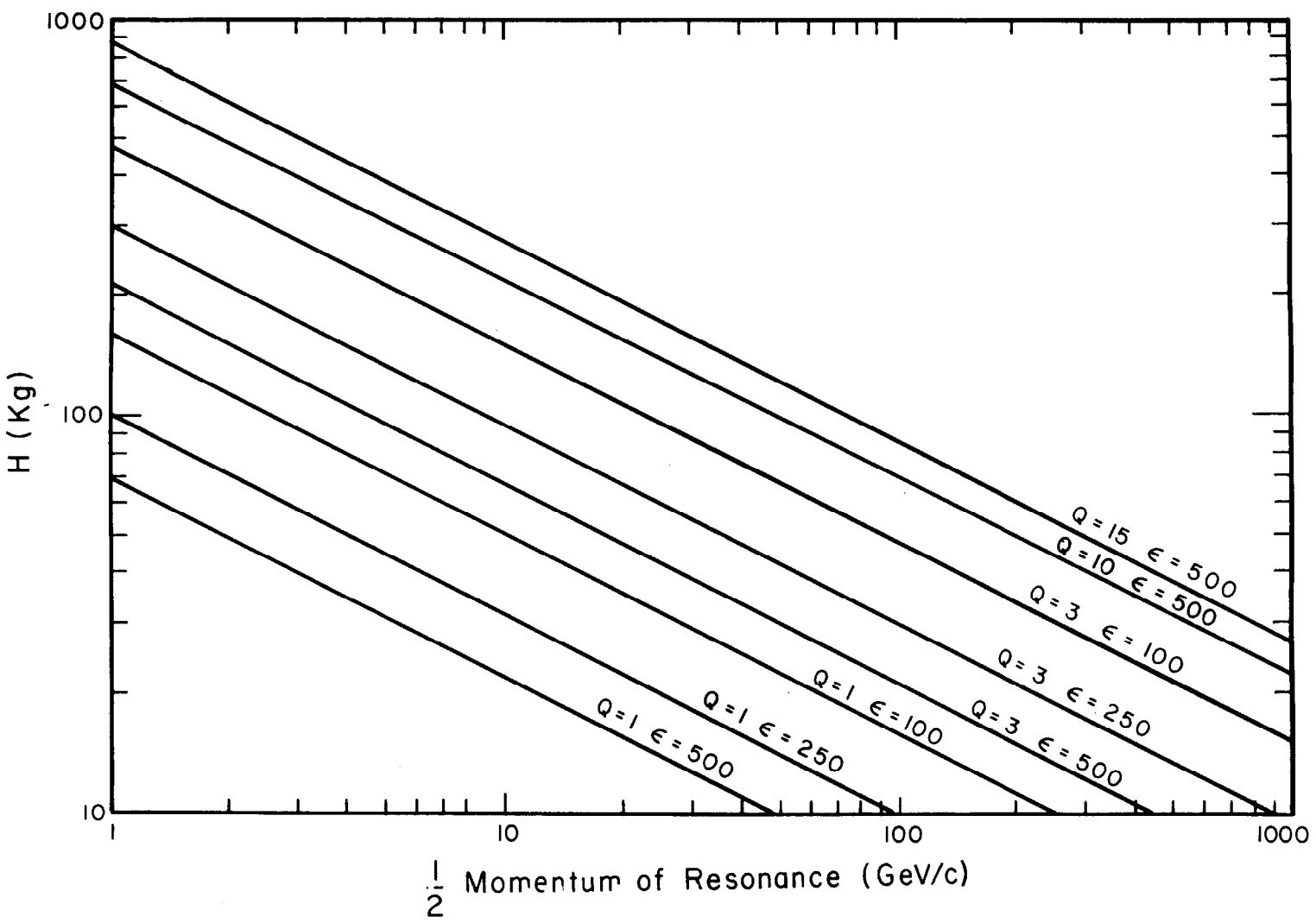


Fig. 7. Optimum magnetic field for matching angle and momentum errors in missing mass measurements as a function of momentum. Q is in GeV/c², setting error ϵ in microns.

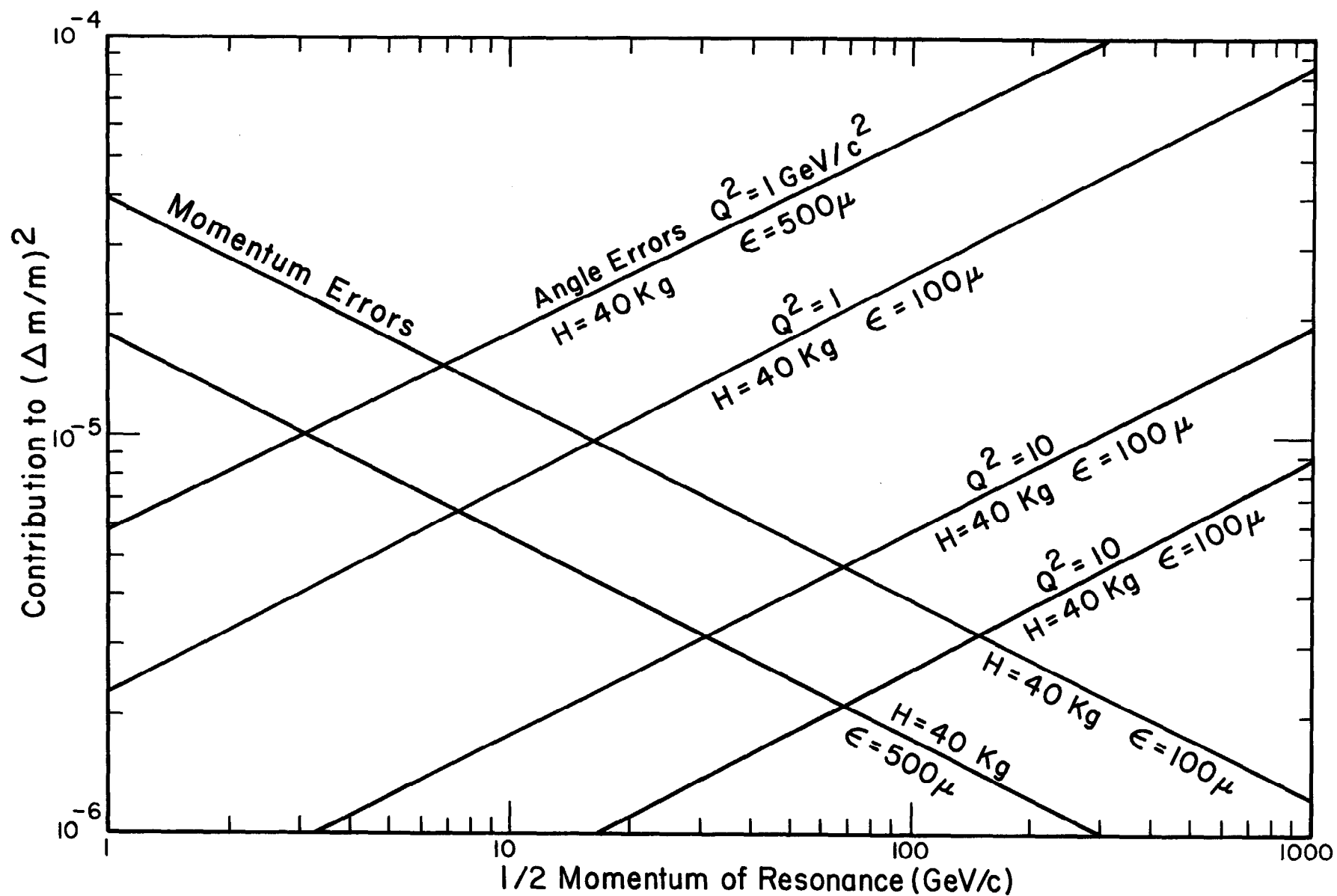


Fig. 8. Contributions of momentum and angle errors to mass measurements. Track length assumed optimum.

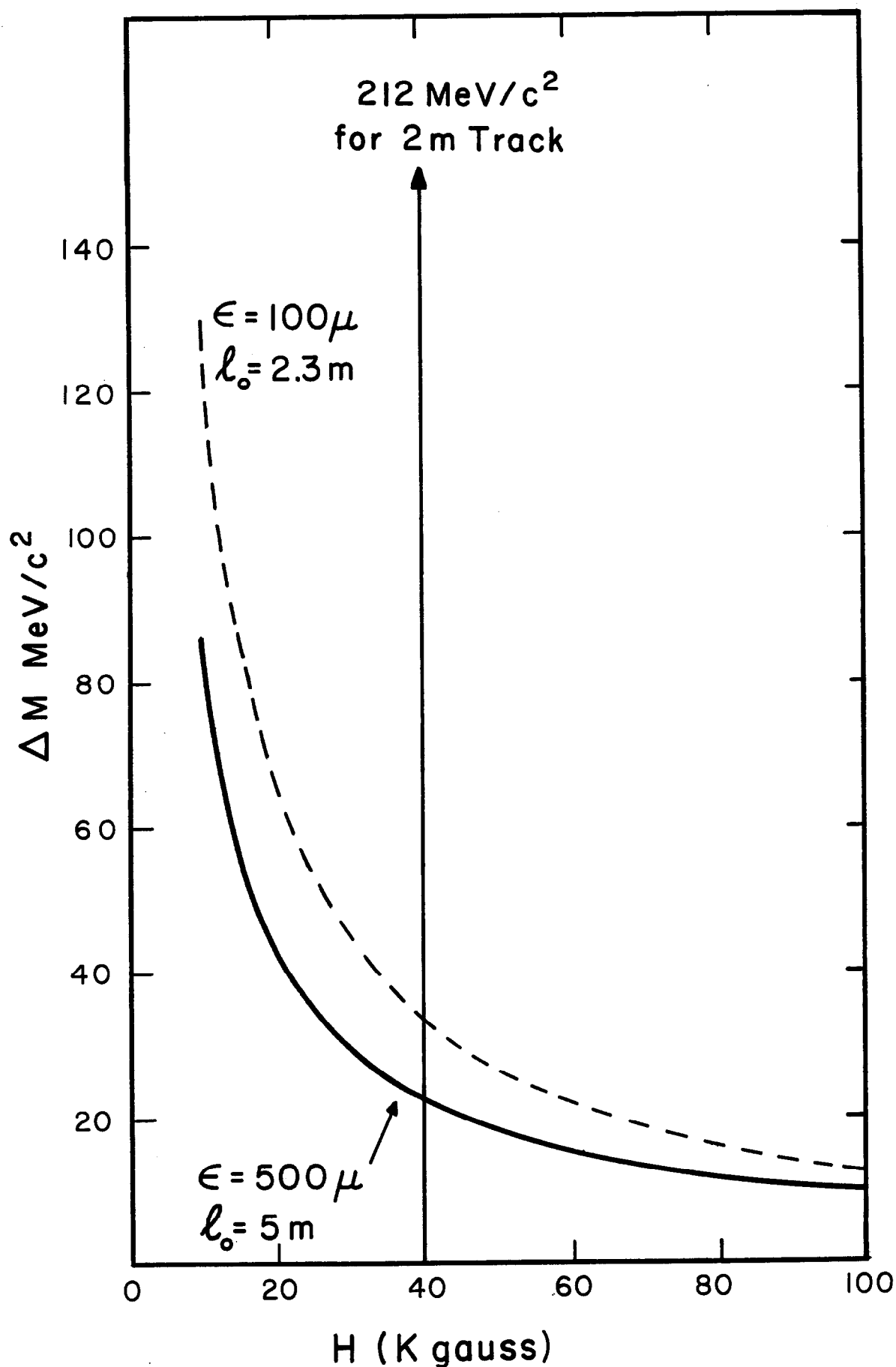


Fig. 9. Mass error vs magnetic field for p-p scattering at 100 GeV/c. Assumed values: $\theta = 15.5$ degrees, $p = 50.5$ GeV/c, $M = 12.76 \text{ GeV}/c^2$